

A model for the dynamics of COVID-19 infection transmission in human with latent delay

Amar N. Chatterjee¹
anchaterji@gmail.com

Teklebirhan Abraha²
tekbir98@yahoo.com

Fahad Al Basir³
fahadbasir@gmail.com

Delfim F. M. Torres^{4*}
delfim@ua.pt

¹Department of Mathematics, K.L.S. College, Nawada, Magadh University, Bodhgaya, Bihar-805110, India

²Department of Mathematics, Aksum University, Aksum, Ethiopia

³Department of Mathematics, Asansol Girls' College, West Bengal 713304, India

⁴R&D Unit CIDMA, Department of Mathematics, University of Aveiro, 3810-193 Aveiro, Portugal

Abstract

In this research, we have derived a mathematical model for within human dynamics of COVID-19 infection using delay differential equations. The new model considers a 'latent period' and 'the time for immune response' as delay parameters, allowing us to study the effects of time delays in human COVID-19 infection. We have determined the equilibrium points and analyzed their stability. The disease-free equilibrium is stable when the basic reproduction number, R_0 , is below unity. Stability switch of the endemic equilibrium occurs through Hopf-bifurcation. This study shows that the effect of latent delay is stabilizing whereas immune response delay has a destabilizing nature.

Keywords: mathematical modeling; time delays; stability; Hopf-bifurcation; numerical simulations.

MSC: 34H20; 34K20; 92-10.

1 Introduction

The world is still suffering from the ongoing pandemic coronavirus disease (COVID-19) caused by the SARS-CoV-2 virus. The outbreak of COVID-19 started in Wuhan China, in December 2019, and now it has been spread over more than 226 countries and territories. COVID-19 is a rapidly spreader infectious disease that threatens the health system of mankind. Infected people experience mild and moderate symptoms and recover without special treatment. However, the worst condition appears for the patient who is suffering from chronic diseases like heart, kidney, and lungs disease. These people become seriously ill and they need medical attention like oxygen support.

The virus is spread from infected person's mouth when they cough, sneeze and speak through droplets. By touching a contaminated surface or by breathing near some COVID-19 infected person, one may be infected. The crowded and indoor environment helps the virus for community's spreading. The World Health Organization (WHO) has approved several COVID-19 vaccines

*This is a preprint of a paper whose final and definite form is published in 'Afrika Matematika' at <https://doi.org/10.1007/s13370-024-01226-0>. Submitted 02-07-2022; Revised 12-09-2024; Accepted 14-12-2024.

*Corresponding author. Email: delfim@ua.pt

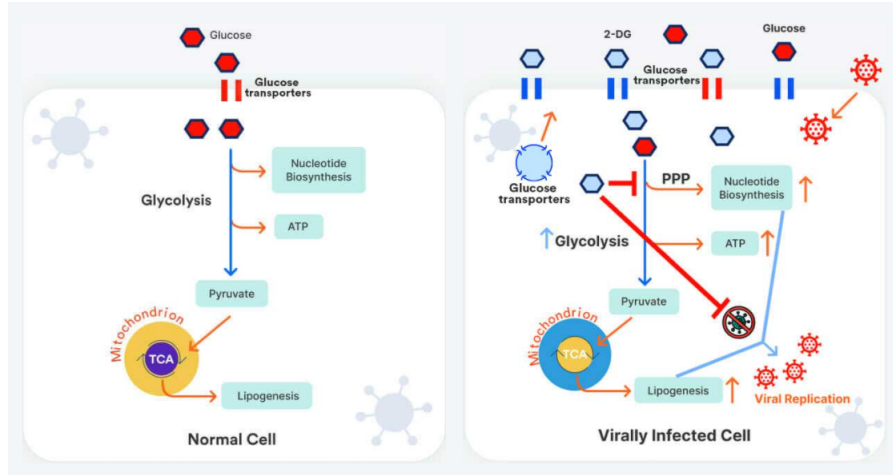


Figure 1: Role of 2-DG – an antiviral effect as it acts on host cells. Source: [1].

and the first mass vaccination program started in early December 2020. The listed vaccines approved by WHO are Pfizer/BioNTech Comirnaty, SII/COVISHIELD, AstraZeneca/AZD1222 vaccines, Janssen/Ad26.COV 2.S, Moderna COVID-19 vaccine (mRNA 1273), Sinopharm COVID-19 vaccine, Sinovac-CoronaVac, and COVAXIN vaccine [2].

In spite of vaccination, some people are being infected by different variants of the SARS-CoV-2 virus. Thus, proper non-pharmaceutical intervention and maintaining Standard Operating Procedures (SOP) can only reduce the chances of reinfection. Recently, The Defence Research Development Organisation (DRDO, India) gave the license to Granules India to manufacture COVID-19 treatment drug, 2-Deoxy-D-Glucose (2-DG). It is an antiviral and anti-inflammatory drug (see Figure 1). Based on Phase II and Phase III trials, 2-DG has received emergency use authorization to be a useful adjunct therapy in moderate COVID-19 patients in the hospital settings.

In the health sector, mathematical models are used to understand the disease dynamics and help for decision-making for controlling the infection [3–5]. Currently, there are many mathematical models used to explain the disease progression of the COVID-19 pandemic, for more details we refer the reader, e.g., to [6–11]. When the COVID-19 has arrived, researchers mainly working on mathematical biology have formulated mathematical models to study the spread of the pandemic, prevention and control of the pandemic, and the influence of prevention of measures [12–18]. The mathematical study of intrahost viral dynamics of COVID-19 infection dynamics plays a pivotal role to develop drugs or vaccines. Also, these studies help us to find the role of the existing drugs against COVID-19 infection. Mathematical modeling with real data contributes to widely discover the dynamical characteristics of an infection at cellular level [7, 19–26].

Tang, Ma and Bai developed a model of virus and host immune response dynamics, incorporating the concentration of DPP4 receptors for MARS-CoV infection [9]. Chatterjee and Basir [27], and Mondal, Samui and Chatterjee [16] studied a mathematical model indicating the dynamical activities of epithelial cells during SARS-CoV-2 infection in the presence of cytotoxic T lymphocytes (CTL) response. Hernandez-Vargas and Velasco-Hernandez described a model in cellular level dynamics of SARS-CoV-2 and T cell responses against the viral replication during the COVID-19 infection [28]. The effect of the several pathogenic characteristics of SARS-CoV-2 and host immune response is studied by Wang et al. [29]. They also evaluated and observed that anti-inflammatory treatment strategies, or a combination of antiviral drugs with interferon, are effective in reducing the plateau phase in viral load [29]. Chatterjee and co-authors proposed a fractional differential equations model in cellular level, accounting the lytic and non-lytic effects of immune response in the kinetics of the model, exploring the effect of a commonly used antiviral drug in COVID-19 treatment, while applying an optimal control-theoretic approach [30, 31]. In the previous models

of COVID-19, time lag was not considered by the researchers. Here, we study the effects of time delays in human COVID-19 infection.

In SARS-CoV-2 infection, the virus life cycle plays a crucial role in disease progression. The binding of a viral particle to a receptor on a target epithelial cell initiates a series of events that can ultimately lead to the target cell becoming productively infected, i.e., producing new virus. In the previous models, it is assumed that the process of infection is instantaneous. In other words, it is assumed that as soon as the virus contacts a target cell, then the cell begins producing virus. However, in reality, there is a time lag between initial viral entry into a cell and the time the cell become virus producing. For this reason, in this work we consider this delay to determine accurately the half life of free virus from drug perturbation experiments. We will show that the delay affects the estimated value for the infected T-cell loss rate when one assumes the drug is not completely effective.

We incorporate the intracellular delay in the model proposed in [27] by assuming a latent delay $\tau_1 > 0$ that means the generation of virus producing cells at time t is due to the infection of target cells at time $(t - \tau_1)$. We also consider an immune response delay $\tau_2 > 0$ to account for the time needed to activate CTL responses, i.e., the CTL response against pathogens at time t were activated by the infected epithelial cells at time $(t - \tau_2)$.

Our study is organized in the following manner. In Section 2, a compartmental model of intrahost immune responses on SARS-CoV-2 viral dynamics is proposed. Then, we modify the proposed model taking into account the presence of delays. Section 3 deals with the analysis of the model, such as non-negativity and boundedness of all the solutions of the system. In Section 4, the delayed induced mathematical model is analysed. Numerical simulations are performed in Section 5 to examine whether the analytical results are associated with the numerical findings or not. Finally, we discuss about our inclusive analytical and numerical results in Section 6.

2 Model derivation

The base model was proposed by Chatterjee and Al Basir [27]. Here, we extend the model in [27] using a saturated infection rate and two time delay factors.

Chatterjee and Al Basir [27] proposed the model considering the interaction between epithelial cells and SARS-CoV-2 virus along with CTL responses over the infected cells. Five populations, namely, the uninfected epithelial cells $T(t)$, infected cells $I(t)$, angiotensin-converting enzyme 2 (ACE2) receptor of the epithelial cells $E(t)$, SARS-CoV-2 virus $V(t)$ and CTLs against the pathogen, denoted as $C(t)$, were considered. Mathematically, the model by Chatterjee and Al Basir is as follows:

$$\begin{cases} \frac{dT}{dt} = \lambda_1 - \beta EVT - d_T T, \\ \frac{dI}{dt} = \beta EVT - d_I I - pIC, \\ \frac{dV}{dt} = m d_I I - d_V V, \\ \frac{dE}{dt} = \lambda_2 - \theta \beta EVT - d_E E, \\ \frac{dC}{dt} = \alpha IC \left(1 - \frac{C}{C_{\max}}\right) - d_c C. \end{cases} \quad (1)$$

It is assumed that the susceptible epithelial cells are produced at a rate λ_1 from the precursor cells and die at a rate d_T . The susceptible cells become infected at a rate $\beta E(t)V(t)T(t)$. The infection rate is inhibited by the nonlytic effect of CTLs at a rate $1 + qC$, where q is the efficacy of the nonlytic effect. The constant d_I is the death rate of the infected epithelial cells. Infected cells are also cleared by the lytic effect of the body's defensive CTLs at a rate pIC , where p is the efficacy of lytic effect. The infected cells produce new viruses at the rate $m d_I$ during their life; and d_V is the death rate of new virions, where m is any positive integer. It is also assumed that

ACE2 is produced from the surface of uninfected epithelial cells at the constant rate λ_2 and the ACE2 is destroyed, when free viruses try to infect uninfected cells, at the rate $\theta\beta E(t)V(t)T(t)$ and is hydrolyzed at the rate $d_E E$. The CTL proliferation, in the presence of infected cells, is described by the term

$$\alpha IC \left(1 - \frac{C}{C_{\max}}\right),$$

which shows the antigen-dependent proliferation. Here, we consider the logistic growth of CTL with C_{\max} as the maximum concentration of CTL and d_C its rate of decay. We now make the following additional considerations to derive the desired model.

As discussed in the Introduction, we incorporate the intracellular delay in the model given by (1) by assuming that the generation of virus producing cells at time t is due to the infection of target cells at time $t - \tau_1$, where τ_1 is a constant. Here $e^{-d_I \tau_1}$ represents the survival probability during the latent time τ_1 .

We also consider an immune delay τ_2 to account for the time needed to activate CTL responses, i.e., the CTL response against pathogens at time t were activated by the infected epithelial cells at time $t - \tau_2$, where τ_2 is constant.

The equations describing this new model are then given by

$$\begin{cases} \frac{dT}{dt} = \lambda_1 - (1 - \epsilon_1) \frac{\beta EVT}{1 + qC} - d_T T, \\ \frac{dI}{dt} = (1 - \epsilon_1) \frac{e^{-d_I \tau_1} \beta E(t - \tau_1) V(t - \tau_1) T(t - \tau_1)}{1 + qC(t - \tau_1)} - d_I I - pIC, \\ \frac{dV}{dt} = (1 - \epsilon_2) m d_I I - d_V V, \\ \frac{dE}{dt} = \lambda_2 - \theta \beta EVT - d_E E, \\ \frac{dC}{dt} = \alpha I(t - \tau_2) C(t - \tau_2) \left(1 - \frac{C(t - \tau_2)}{C_{\max}}\right) - d_C C, \end{cases} \quad (2)$$

where τ_1 and τ_2 are the latent and the immune delays, respectively. A short description of the model parameters and their values is shown in Table 1.

Table 1: Description of the parameters of the proposed model (2) with the values used for numerical simulations.

Parameters	Description	Value
λ_1	Production rate of uninfected cell	5
λ_2	Production rate of ACE2	1
β	Disease transmission rate	0.0001
θ	Bonding rate of ACE2	0.2
d_T	Death rate of uninfected cells	0.1
d_I	Death rate of infected cells	0.1
d_V	Removal rate of virus	0.1
d_E	Hydrolyzing rate of epithelial cells	0.1
d_c	Decay rate of CTL	0.1
p	Killing rate of infected cells by CTL	0.01
m	Number of new virions produced	20
α	Proliferation rate of CTL	0.22
C_{\max}	Maximum proliferation of CTL	100

3 Analysis of the Model without delay

In this section, we analyze the dynamics of the system without delays, i.e., system (1). We derive the basic reproduction number for the system and the stability of equilibria is discussed using this threshold.

3.1 Existence of equilibria

Model (1) has three steady states, namely, (i) the disease-free equilibrium, $E_0 \left(\frac{\lambda_1}{d_T}, 0, 0, \frac{\lambda_2}{d_E}, 0 \right)$, (ii) the CTL response-free equilibrium $E_1(\tilde{T}, \tilde{I}, \tilde{V}, \tilde{E}, 0)$, where

$$\begin{aligned}\tilde{T} &= \frac{d_V}{\beta m \tilde{E}}, \\ \tilde{I} &= \frac{\beta m \lambda_1 \tilde{E} - d_T d_V}{\beta m d_I \tilde{E}}, \\ \tilde{V} &= \frac{\beta m \lambda_1 - d_T d_V \tilde{E}}{\beta d_V \tilde{E}}, \\ \tilde{E} &= \frac{-(\beta m \theta \lambda_1 - \beta m \lambda_2) + \sqrt{(\beta m \theta \lambda_1 - \beta m \lambda_2)^2 + 4 d_E \beta m \theta d_T d_V}}{2 \beta m d_E},\end{aligned}$$

and (iii) the endemic equilibrium E^* which is given by

$$\begin{aligned}T^* &= \frac{\lambda_1 \alpha - \alpha p C_{\max} I^* - d_I \alpha I^* + p C_{\max} d_c}{\alpha d_T}, \\ V^* &= \frac{m d_I I^*}{d_V}, \\ E^* &= \frac{\lambda_2 \alpha^2 I^* - \theta (\alpha I^* + q (\alpha I^* - d_c) C_{\max}) (\alpha d_I + p (\alpha I^* - d_c) C_{\max})}{\alpha^2 d_E I^*}, \\ C^* &= \frac{C_{\max} (\alpha I^* - d_c)}{\alpha I^*},\end{aligned}$$

where I^* is the positive root of the fourth degree equation

$$a_0 I^4 + a_1 I^3 + a_2 I^2 + a_3 I + a_4 = 0 \quad (3)$$

with

$$\begin{aligned}a_0 &= \alpha^3 \beta m \theta d_Z (p C_{\max} + d_Z)^2 (q C_{\max} + 1), \\ a_1 &= - (3 p q \theta d_c C_{\max}^2 + \theta (\alpha q \lambda_1 + q d_Z d_c + 2 p d_c) C_{\max} + \alpha (\theta \lambda_1 + \lambda_2)) d_Z m \alpha^2 (p C_{\max} + d_Z) \beta, \\ a_2 &= 2 d_Z m q \alpha C_{\max}^2 p d_c ((3/2 p C_{\max} + d_Z) d_c + \lambda_1 \alpha) \theta \beta \\ &\quad + (-C_{\max} p q \alpha^2 d_E d_T d_V + m d_Z d_c \lambda_1 \beta \theta (q d_Z + p) \alpha + m d_Z d_c^2 C_{\max} p^2 \beta \theta) \alpha C_{\max} \\ &\quad + \alpha^2 (((-q C_{\max} d_E d_T d_V + \beta m \lambda_1 \lambda_2 - d_E d_T d_V) d_Z - C_{\max} p d_E d_T d_V) \alpha + m d_c C_{\max} \lambda_2 p \beta d_Z), \\ a_3 &= - (m d_Z d_c^2 C_{\max}^2 p^2 q \beta \theta + p q \alpha (\beta m \theta d_Z d_c \lambda_1 - 2 \alpha d_E d_T d_V) C_{\max} - \alpha^2 d_E d_T d_V (q d_Z + p)) d_c C_{\max}, \\ a_4 &= - \alpha p q C_{\max}^2 d_E d_T d_V d_c^2.\end{aligned}$$

Remark 1. We have $a_0 > 0$ and $a_4 < 0$. Thus, equation (3) has at least one positive real root. For a feasible endemic equilibrium, we also need

$$\frac{d_c}{\alpha} < I^* < \min \left\{ \frac{\lambda_1 \alpha + p d_c C_{\max}}{\alpha (p C_{\max} + d_I)}, \frac{\alpha d_I + q d_c C_{\max}}{\theta \alpha - \theta \alpha q C_{\max} - \lambda^2 \alpha^2} \right\}.$$

3.2 Stability of the equilibria

For the stability of equilibria, we need the nature of the roots of the characteristic equation of the Jacobian matrix at any equilibrium point $E(T, I, V, E, C)$ [32]. We linearize the system (1) using the Jacobian technique. The basic threshold number R_0 of system (1) is defined by the spectral radius of the matrix FV^{-1} , and is given by [33]:

$$R_0 = \frac{m\beta \lambda_1 \lambda_2}{d_V d_E d_T}. \quad (4)$$

The Jacobian matrix of the system (1) at any equilibrium point $E(T, I, V, E, C)$ is given by

$$J(E) = \begin{bmatrix} -\frac{\beta EV}{Cq+1} - d_T & 0 & -\frac{\beta ET}{Cq+1} & -\frac{\beta VT}{Cq+1} & \frac{\beta EVTq}{(Cq+1)^2} \\ \frac{\beta EV}{Cq+1} & -Cp - d_I & \frac{\beta ET}{Cq+1} & \frac{\beta VT}{Cq+1} & -\frac{\beta EVTq}{(Cq+1)^2} - pZ \\ 0 & md_I & -d_V & 0 & 0 \\ -\theta \beta EV & 0 & -\beta ET\theta & -\beta VT\theta - d_E & 0 \\ 0 & \alpha C \left(1 - \frac{C}{C_{\max}}\right) & 0 & 0 & \alpha I \left(1 - \frac{2}{C} C_{\max}\right) - d_c \end{bmatrix}. \quad (5)$$

Theorem 2. *The disease free equilibrium $E_0 \left(\frac{\lambda_1}{d_T}, 0, 0, \frac{\lambda_2}{d_E}, 0\right)$ is stable for $R_0 < 1$ and unstable for $R_0 > 1$.*

Proof. From (5), the Jacobian matrix at the disease-free equilibrium point $E_0 \left(\frac{\lambda_1}{d_T}, 0, 0, \frac{\lambda_2}{d_E}, 0\right)$ is given by

$$J(E_0) = \begin{bmatrix} -d_T & 0 & -\frac{\beta \lambda_1 \lambda_2}{d_T d_E} & 0 & 0 \\ 0 & -d_I & \frac{\beta \lambda_1 \lambda_2}{d_T d_E} & 0 & 0 \\ 0 & md_I & -d_V & 0 & 0 \\ 0 & 0 & -\frac{\beta \lambda_1 \lambda_2 \theta}{d_T d_E} & -d_E & 0 \\ 0 & 0 & 0 & 0 & -d_c \end{bmatrix},$$

whose characteristic equation in ρ is given by

$$|\rho I - J(E_0)| = \begin{vmatrix} \rho + d_T & 0 & \frac{\beta \lambda_1 \lambda_2}{d_T d_E} & 0 & 0 \\ 0 & \rho + d_I & -\frac{\beta \lambda_1 \lambda_2}{d_T d_E} & 0 & 0 \\ 0 & -md_I & \rho + d_V & 0 & 0 \\ 0 & 0 & \frac{\beta \lambda_1 \lambda_2 \theta}{d_T d_E} & \rho + d_E & 0 \\ 0 & 0 & 0 & 0 & \rho + d_c \end{vmatrix} = 0.$$

From this we obtain that

$$(\rho + d_T)(\rho + d_E)(\rho + d_c) [\rho^2 + (d_V + d_I)\rho + d_E d_T d_V d_I - \beta \lambda_1 \lambda_2 m d_I] = 0. \quad (6)$$

Hence, using the Routh–Hurwitz criterion, we conclude that E_0 is stable if and only if

$$d_V d_E d_T > m\beta \lambda_1 \lambda_2,$$

which is equivalent to $R_0 < 1$. \square

Theorem 3. *The CTL-free equilibrium, $E_1(\tilde{T}, \tilde{I}, \tilde{V}, \tilde{E}, 0)$, is asymptotically stable if and only if the following conditions are satisfied:*

$$\begin{aligned}\alpha_1 &> 0, \\ \alpha_2 &> 0, \\ \alpha_3 &> 0, \\ \alpha_4 &> 0, \\ \alpha_1 \alpha_2 - \alpha_3 &> 0, \\ (\alpha_1 \alpha_2 - \alpha_3) \alpha_3 - \alpha_1^2 \alpha_4 &> 0,\end{aligned}$$

where

$$\begin{aligned}\alpha_1 &= -a_{33} - a_{44} - a_{11} - a_{22}, \\ \alpha_2 &= (a_{33} + a_{44} + a_{22}) a_{11} - a_{23} a_{32} + (a_{33} + a_{22}) a_{44} + a_{33} a_{22} - a_{41} a_{14}, \\ \alpha_3 &= (a_{23} a_{32} + (-a_{33} - a_{22}) a_{44} - a_{33} a_{22}) a_{11} \\ &\quad + (-a_{13} a_{21} + a_{23} a_{44} - a_{24} a_{43}) a_{32} - a_{33} a_{22} a_{44} + a_{41} a_{14} (a_{33} + a_{22}), \\ \alpha_4 &= ((-a_{23} a_{44} + a_{24} a_{43}) a_{32} + a_{33} a_{22} a_{44}) a_{11} \\ &\quad + (a_{21} a_{13} a_{44} + (-a_{21} a_{43} + a_{23} a_{41}) a_{14} - a_{41} a_{13} a_{24}) a_{32} - a_{33} a_{41} a_{14} a_{22},\end{aligned}\tag{7}$$

with

$$\begin{aligned}a_{11} &= -\beta EV - d_T, & a_{21} &= \beta EV, & a_{41} &= -\theta \beta EV, \\ a_{22} &= -d_I, & a_{32} &= m d_I, \\ a_{13} &= -\beta ET, & a_{23} &= \beta ET, & a_{33} &= -d_V, & a_{43} &= -\beta \theta ET, \\ a_{14} &= -\beta ET, & a_{24} &= \beta ET, & a_{44} &= -d_V, & a_{43} &= -\beta \theta ET, \\ a_{15} &= \beta EVTq, & a_{25} &= -\beta EVTq - pI, & a_{55} &= -d_c.\end{aligned}\tag{8}$$

Proof. Using (5), the Jacobian matrix of (1) at $E_1(\tilde{T}, \tilde{I}, \tilde{V}, \tilde{E}, 0)$ is given by

$$J(E_1) = \begin{bmatrix} a_{11} & 0 & a_{13} & a_{14} & a_{15} \\ a_{21} & a_{22} & a_{23} & a_{24} & a_{25} \\ 0 & a_{32} & a_{33} & 0 & 0 \\ a_{41} & 0 & a_{43} & a_{44} & 0 \\ 0 & 0 & 0 & 0 & a_{55} \end{bmatrix},$$

with the a_{ij} given by (8), whose characteristic equation in ρ is

$$(\rho - a_{55}) (\rho^4 + \alpha_1 \rho^3 + \alpha_2 \rho^2 + \alpha_3 \rho + \alpha_4) = 0,\tag{9}$$

with the α_i , $i = 1, \dots, 4$, given by (7). Here, one eigenvalue is $-d_c$ and the rest of the eigenvalues satisfy the following equation:

$$\rho^4 + \alpha_1 \rho^3 + \alpha_2 \rho^2 + \alpha_3 \rho + \alpha_4 = 0.$$

Hence, using the Routh–Hurwitz criterion, we arrive to the intended result. \square

Theorem 4. *The coexisting equilibrium E^* is asymptotically stable if and only if the following conditions are satisfied:*

$$\begin{aligned}B_5 &> 0, \\ B_1 B_2 - B_3 &> 0, \\ B_3(B_1 B_2 - B_3) - B_1(B_1 B_4 - B_5) &> 0, \\ (B_1 B_2 - B_3)(B_3 B_4 - B_2 B_5) - (B_1 B_4 - B_5)^2 &> 0,\end{aligned}\tag{10}$$

where

$$\begin{aligned}
B_1 &= -b_{33} - b_{44} - b_{55} - b_{11} - b_{22}, \\
B_2 &= (b_{33} + b_{44} + b_{11} + b_{22}) b_{55} + (b_{44} + b_{11} + b_{22}) b_{33} + (b_{11} + b_{22}) b_{44} \\
&\quad - b_{22} b_{11} - b_{14} b_{41} - b_{23} b_{32} + b_{25} b_{52}, \\
B_3 &= ((-b_{44} - b_{11} - b_{22}) b_{33} + (-b_{11} - b_{22}) b_{44} + b_{23} b_{32} + b_{14} b_{41} - b_{22} b_{11}) b_{55}, \\
&\quad + ((-b_{11} - b_{22}) b_{44} + b_{25} b_{52} + b_{14} b_{41} - b_{22} b_{11}) b_{33} + (-b_{22} b_{11} + b_{23} b_{32} + b_{25} b_{52}) b_{44} \\
&\quad + (b_{23} b_{32} + b_{25} b_{52}) b_{11} + (-b_{13} b_{21} - b_{24} b_{43}) b_{32} + b_{41} b_{14} b_{22} - b_{52} b_{15} b_{21}, \\
B_4 &= \left((b_{11} + b_{22}) b_{44} - b_{14} b_{41} + b_{22} b_{11} \right) b_{33} \\
&\quad + (b_{22} b_{11} - b_{23} b_{32}) b_{44} - b_{23} b_{32} b_{11} + (b_{13} b_{21} + b_{24} b_{43}) b_{32} - b_{41} b_{14} b_{22} \Big) b_{55} \\
&\quad + ((b_{22} b_{11} - b_{25} b_{52}) b_{44} - b_{25} b_{52} b_{11} - b_{41} b_{14} b_{22} + b_{52} b_{15} b_{21}) b_{33} \\
&\quad + ((-b_{23} b_{32} - b_{25} b_{52}) b_{11} + b_{21} (b_{13} b_{32} + b_{15} b_{52})) b_{44}, \\
B_5 &= \left(b_{22} (-b_{11} b_{44} + b_{14} b_{41}) b_{33} + b_{32} ((b_{11} b_{23} - b_{13} b_{21}) b_{44} - b_{24} b_{43} b_{11} + (b_{13} b_{24} - b_{14} b_{23}) b_{41}) \right) b_{55} \\
&\quad + (b_{43} b_{14} b_{21}) b_{55} - b_{52} ((-b_{11} b_{25} + b_{15} b_{21}) b_{44} + b_{41} (b_{14} b_{25} - b_{15} b_{24})) b_{33},
\end{aligned} \tag{11}$$

with the coefficients b_{ij} given by

$$\begin{aligned}
b_{11} &= -\frac{EV\beta}{Cq+1} - d_T, & b_{21} &= \frac{EV\beta}{Cq+1}, & b_{41} &= -\theta\beta EV, \\
b_{22} &= -Cp - d_Z, & b_{32} &= md_I, & b_{52} &= \alpha C \left(1 - \frac{C}{C_{\max}} \right), \\
b_{13} &= -\frac{\beta ET}{Cq+1}, & b_{23} &= \frac{\beta ET}{Cq+1}, & b_{33} &= -d_V, & b_{43} &= -\beta\theta ET, \\
b_{14} &= -\frac{\beta VT}{Cq+1}, & b_{24} &= \frac{\beta VT}{Cq+1}, & b_{44} &= -TV\beta\theta - d_E, \\
b_{15} &= \frac{\beta EVTq}{(Cq+1)^2}, & b_{25} &= -\frac{\beta EVTq}{(Cq+1)^2} - pZ, & b_{55} &= -\frac{\alpha Z(-C_{\max} + 2C)}{C_{\max}} - d_c.
\end{aligned} \tag{12}$$

Proof. Using (5), the Jacobian matrix of (1) at the coexistence equilibrium point E^* is given as

$$J(E^*) = \begin{bmatrix} b_{11} & 0 & b_{13} & b_{14} & b_{15} \\ b_{21} & b_{22} & b_{23} & b_{24} & b_{25} \\ 0 & b_{32} & b_{33} & 0 & 0 \\ b_{41} & 0 & b_{43} & b_{44} & 0 \\ 0 & b_{52} & 0 & 0 & b_{55} \end{bmatrix},$$

with the b_{ij} given in (12), whose characteristic equation in ρ is given by

$$\rho^5 + B_1\rho^4 + B_2\rho^3 + B_3\rho^2 + B_4\rho + B_5 = 0 \tag{13}$$

with B_i , $i = 1, \dots, 5$, given by (11). Hence, using the Routh–Hurwitz criterion, all roots of the characteristic equation (13) have negative real parts, provided the conditions (10) hold. \square

4 Analysis of the model with delays

Let ψ denote the Banach space of continuous functions $\psi : [-\tau, 0] \rightarrow \mathbb{R}^5$ equipped with the sup-norm

$$\|\psi\| = \sup_{-\tau \leq \theta \leq 0} \{|\psi_1(\theta)|, |\psi_2(\theta)|, |\psi_3(\theta)|, |\psi_4(\theta)|, |\psi_5(\theta)|\}.$$

For biological reasons, populations always have non-negative values. Therefore, the initial functions for our model (2) are given as below [33]:

$$\begin{cases} T(\theta) = \psi_1(\theta), & I(\theta) = \psi_2(\theta), & V(\theta) = \psi_3(\theta), & E(\theta) = \psi_4(\theta), & C(\theta) = \psi_5(\theta), \\ \psi_i(\theta) \geq 0, & \theta \in [-\tau, 0], & \psi_i(0) > 0, & \psi = (\psi_1, \psi_2, \psi_3, \psi_4, \psi_5) \in \mathcal{C}([-\tau, 0], \mathbb{R}_+^5), \end{cases} \quad (14)$$

where $\tau = \max\{\tau_1, \tau_2\}$ and $\mathbb{R}_+^5 = \{(x_1, x_2, x_3, x_4, x_5) \mid x_i \geq 0, i = 1, 2, 3, 4, 5\}$. The system (2) exhibits three equilibrium points: (i) the disease-free equilibrium, $E_0\left(\frac{\lambda_1}{d_T}, 0, 0, \frac{\lambda_2}{d_E}, 0\right)$, (ii) the CTL response-free equilibrium $E_1(\tilde{T}, \tilde{I}, \tilde{V}, \tilde{E}, 0)$, where

$$\begin{aligned} \tilde{T} &= \frac{d_V}{E\beta m(\epsilon_1\epsilon_2 - \epsilon_1 - \epsilon_2 + 1)}, \\ \tilde{I} &= \frac{Em\beta(\epsilon_2 - 1)(\epsilon_1 - 1)\lambda_1(1 - \epsilon_1) - d_T d_V}{E\beta m d_Z(\epsilon_2 - 1)}, \\ \tilde{V} &= \frac{Em\beta(\epsilon_2 - 1)(\epsilon_1 - 1)\lambda_1(1 - \epsilon_1) - d_T d_V}{E\beta d_V}, \end{aligned}$$

and \tilde{E} is the positive solution of $\lambda_2 - \frac{\theta(Em\beta(\epsilon_2 - 1)(\epsilon_1 - 1)\lambda_1(1 - \epsilon_1) - d_T d_V)}{Em\beta(\epsilon_2\epsilon_1 - \epsilon_1 - \epsilon_2 + 1)} - d_E E = 0$, and (iii) the endemic equilibrium E^* , which is the positive solution of the nonlinear system

$$\begin{cases} \lambda_1 - (1 - \epsilon_1)\frac{\beta EVT}{1 + qC} - d_T T = 0, \\ (1 - \epsilon_1)\frac{e^{-d_I \tau_1} \beta E(t - \tau_1) V(t - \tau_1) T(t - \tau_1)}{1 + qC(t - \tau_1)} - d_I I - pIC = 0, \\ (1 - \epsilon_2)md_I I - d_V V = 0, \\ \lambda_2 - \theta\beta EVT - d_E E = 0, \\ \alpha I(t - \tau_2)C(t - \tau_2)\left(1 - \frac{C(t - \tau_2)}{C_{\max}}\right) - d_c C = 0. \end{cases}$$

If we linearize our system (2) about a steady state $E(T, I, V, E, C)$, we obtain that

$$\frac{dX}{dt} = FX(t) + GX(t - \tau_1) + HX(t - \tau_2). \quad (15)$$

Here, F , G and H are 5×5 matrices given as

$$F = [F_{ij}] = \begin{bmatrix} -\frac{\beta EV}{qC+1} - d_T & 0 & -\frac{\beta ET}{qC+1} & -\frac{\beta VT}{qC+1} & \frac{\beta EVTq}{(qC+1)^2} \\ \frac{(1-\epsilon_1)\beta EV}{qC+1} & -pC - d_I & \frac{(1-\epsilon_1)\beta ET}{qC+1} & \frac{(1-\epsilon_1)\beta VT}{qC+1} & -\frac{(1-\epsilon_1)\beta qEVT}{(qC+1)^2} - pI \\ 0 & (1 - \epsilon_2)md_I & -d_V & 0 & 0 \\ -\theta\beta EV & 0 & -\beta ET\theta & -\beta VT\theta - d_E & 0 \\ 0 & 0 & 0 & 0 & -d_c \end{bmatrix},$$

$$G = [G_{ij}] = \begin{bmatrix} 0 & 0 & 0 & 0 & 0 \\ \frac{(1-\epsilon_1)e^{-d_I\tau_1}\beta EV}{1+qC} & 0 & \frac{(1-\epsilon_1)e^{-d_I\tau_1}\beta ET}{1+qC} & \frac{(1-\epsilon_1)e^{-d_I\tau_1}\beta VT}{1+qC} & -\frac{(1-\epsilon_1)e^{-d_I\tau_1}\beta EVT}{(qC+1)^2} \\ 0 & 0 & 0 & 0 & 0 \\ 0 & 0 & 0 & 0 & 0 \\ 0 & 0 & 0 & 0 & 0 \end{bmatrix},$$

$$H = [H_{ij}] = \begin{bmatrix} 0 & 0 & 0 & 0 & 0 \\ 0 & 0 & 0 & 0 & 0 \\ 0 & 0 & 0 & 0 & 0 \\ 0 & 0 & 0 & 0 & 0 \\ 0 & \alpha C(1 - \frac{C}{C_{\max}}) & 0 & 0 & \alpha I(1 - \frac{2C}{C_{\max}}) \end{bmatrix}.$$

The characteristic equation of the delayed system (2) then becomes

$$\Delta(\xi, \tau_1, \tau_2) = |\xi I - F - e^{-\xi\tau_1}G - e^{-\xi\tau_2}H| = 0.$$

This yields the characteristic equation

$$\begin{aligned} 0 = & \xi^5 + L_1\xi^4 + L_2\xi^3 + L_3\xi^2 + L_4\xi + L_5 + e^{-\xi\tau_1}(\xi^4 + M_2\xi^3 + M_3\xi^2 + M_4\xi + M_5) \\ & + e^{-\xi\tau_2}(\xi^5 + K_1\xi^4 + K_2\xi^3 + K_3\xi^2 + K_4\xi + K_5) + e^{-\xi(\tau_1+\tau_2)}(\xi^4 + Q_2\xi^3 + Q_3\xi^2 + Q_4\xi + Q_5), \end{aligned} \quad (16)$$

where the coefficients are given by

$$\begin{aligned} L_1 &= -F_{11} - F_{22} - F_{33} - F_{44} - F_{55}, \\ L_2 &= +F_{11}F_{22} - F_{23}F_{32} + F_{11}F_{33} + F_{22}F_{33} - F_{14}F_{41} + F_{11}F_{44} \\ &\quad + F_{22}F_{44} + F_{33}F_{44} + F_{11}F_{55} + F_{22}F_{55} + F_{33}F_{55} + F_{44}F_{55}, \\ L_3 &= -F_{13}F_{21}F_{32} + F_{11}F_{23}F_{32} - F_{11}F_{22}F_{33} + F_{14}F_{22}F_{41} \\ &\quad + F_{14}F_{33}F_{41} - F_{24}F_{32}F_{43} - F_{11}F_{22}F_{44} \\ &\quad + F_{23}F_{32}F_{44} - F_{11}F_{33}F_{44} - F_{22}F_{33}F_{44} \\ &\quad - F_{11}F_{22}F_{55} + F_{23}F_{32}F_{55} - F_{11}F_{33}F_{55} \\ &\quad - F_{22}F_{33}F_{55} + F_{14}F_{41}F_{55} - F_{11}F_{44}F_{55} \\ &\quad - F_{22}F_{44}F_{55} - F_{33}F_{44}F_{55}, \\ L_4 &= +F_{14}F_{23}F_{32}F_{41} - F_{13}F_{24}F_{32}F_{41} - F_{14}F_{22}F_{33}F_{41} \\ &\quad - F_{14}F_{21}F_{32}F_{43} + F_{11}F_{24}F_{32}F_{43} + F_{13}F_{21}F_{32}F_{44} \\ &\quad - F_{11}F_{23}F_{32}F_{44} + F_{11}F_{22}F_{33}F_{44} + F_{13}F_{21}F_{32}F_{55} \\ &\quad - F_{11}F_{23}F_{32}F_{55} + F_{11}F_{22}F_{33}F_{55} - F_{14}F_{22}F_{41}F_{55} \\ &\quad - F_{14}F_{33}F_{41}F_{55} + F_{24}F_{32}F_{43}F_{55} + F_{11}F_{22}F_{44}F_{55} \\ &\quad - F_{23}F_{32}F_{44}F_{55} + F_{11}F_{33}F_{44}F_{55} + F_{22}F_{33}F_{44}F_{55}, \\ L_5 &= -F_{14}F_{23}F_{32}F_{41}F_{55} + F_{13}F_{24}F_{32}F_{41}F_{55} + F_{14}F_{22}F_{33}F_{41}F_{55} \\ &\quad + F_{14}F_{21}F_{32}F_{43}F_{55} - F_{11}F_{24}F_{32}F_{43}F_{55} - F_{13}F_{21}F_{32}F_{44}F_{55} \\ &\quad + F_{11}F_{23}F_{32}F_{44}F_{55} - F_{11}F_{22}F_{33}F_{44}F_{55}, \\ M_2 &= -F_{32}G_{23}, \\ M_3 &= -F_{13}F_{32}G_{21} + F_{11}F_{32}G_{23} + F_{32}F_{44}G_{23} + F_{32}F_{55}G_{23} - F_{32}F_{43}G_{24}, \\ M_4 &= -F_{14}F_{32}F_{43}G_{21} + F_{13}F_{32}F_{44}G_{21} + F_{13}F_{32}F_{55}G_{21} \\ &\quad + F_{14}F_{32}F_{41}G_{23} - F_{11}F_{32}F_{44}G_{23} - F_{11}F_{32}F_{55}G_{23} \\ &\quad - F_{32}F_{44}F_{55}G_{23} - F_{13}F_{32}F_{41}G_{24} + F_{11}F_{32}F_{43}G_{24} + F_{32}F_{43}F_{55}G_{24}, \\ M_5 &= +F_{14}F_{32}F_{43}F_{55}G_{21} - F_{13}F_{32}F_{44}F_{55}G_{21} - F_{14}F_{32}F_{41}F_{55}G_{23} \\ &\quad + F_{11}F_{32}F_{44}F_{55}G_{23} + F_{13}F_{32}F_{41}F_{55}G_{24} - F_{11}F_{32}F_{43}F_{55}G_{24}, \end{aligned}$$

$$\begin{aligned}
K_1 &= -H_{55}, \\
K_2 &= -F_{25}H_{52} + F_{11}H_{55} + F_{22}H_{55} + F_{33}H_{55} + F_{44}H_{55}, \\
K_3 &= -F_{15}F_{21}H_{52} + F_{11}F_{25}H_{52} + F_{25}F_{33}H_{52} + F_{25}F_{44}H_{52} \\
&\quad - F_{11}F_{22}H_{55} + F_{23}F_{32}H_{55} - F_{11}F_{33}H_{55} \\
&\quad - F_{22}F_{33}H_{55} + F_{14}F_{41}H_{55} - F_{11}F_{44}H_{55} \\
&\quad - F_{22}F_{44}H_{55} - F_{33}F_{44}H_{55}, \\
K_4 &= +F_{15}F_{21}F_{33}H_{52} - F_{11}F_{25}F_{33}H_{52} \\
&\quad - F_{15}F_{24}F_{41}H_{52} + F_{14}F_{25}F_{41}H_{52} + F_{15}F_{21}F_{44}H_{52} \\
&\quad - F_{11}F_{25}F_{44}H_{52} - F_{25}F_{33}F_{44}H_{52} + F_{13}F_{21}F_{32}H_{55} - F_{11}F_{23}F_{32}H_{55} \\
&\quad + F_{11}F_{22}F_{33}H_{55} - F_{14}F_{22}F_{41}H_{55} - F_{14}F_{33}F_{41}H_{55} + F_{24}F_{32}F_{43}H_{55} \\
&\quad + F_{11}F_{22}F_{44}H_{55} - F_{23}F_{32}F_{44}H_{55} + F_{11}F_{33}F_{44}H_{55} + F_{22}F_{33}F_{44}H_{55}, \\
K_5 &= F_{15}F_{24}F_{33}F_{41}H_{52} - F_{14}F_{25}F_{33}F_{41}H_{52} - F_{15}F_{21}F_{33}F_{44}H_{52} + F_{11}F_{25}F_{33}F_{44}H_{52} \\
&\quad - F_{14}F_{23}F_{32}F_{41}H_{55} + F_{13}F_{24}F_{32}F_{41}H_{55} \\
&\quad + F_{14}F_{22}F_{33}F_{41}H_{55} + F_{14}F_{21}F_{32}F_{43}H_{55} - F_{11}F_{24}F_{32}F_{43}H_{55} \\
&\quad - F_{13}F_{21}F_{32}F_{44}H_{55} + F_{11}F_{23}F_{32}F_{44}H_{55} - F_{11}F_{22}F_{33}F_{44}H_{55},
\end{aligned}$$

and

$$\begin{aligned}
Q_2 &= -G_{25}H_{52}, \\
Q_3 &= -F_{15}G_{21}H_{52} + F_{11}G_{25}H_{52} + F_{33}G_{25}H_{52} + F_{44}G_{25}H_{52} + F_{32}G_{23}H_{55}, \\
Q_4 &= +F_{15}F_{33}G_{21}H_{52} + F_{15}F_{44}G_{21}H_{52} - F_{15}F_{41}G_{24}H_{52} - F_{11}F_{33}G_{25}H_{52} \\
&\quad + F_{14}F_{41}G_{25}H_{52} - F_{11}F_{44}G_{25}H_{52} - F_{33}F_{44}G_{25}H_{52} + F_{13}F_{32}G_{21}H_{55} \\
&\quad - F_{11}F_{32}G_{23}H_{55} - F_{32}F_{44}G_{23}H_{55} + F_{32}F_{43}G_{24}H_{55}, \\
Q_5 &= -F_{15}F_{33}F_{44}G_{21}H_{52} + F_{15}F_{33}F_{41}G_{24}H_{52} + F_{11}F_{33}F_{44}G_{25}H_{52} \\
&\quad + F_{14}F_{32}F_{43}G_{21}H_{55} - F_{13}F_{32}F_{44}G_{21}H_{55} - F_{14}F_{32}F_{41}G_{23}H_{55} \\
&\quad + F_{11}F_{32}F_{44}G_{23}H_{55} + F_{13}F_{32}F_{41}G_{24}H_{55} - F_{11}F_{32}F_{43}G_{24}H_{55} - F_{14}F_{33}F_{41}G_{25}H_{52}.
\end{aligned}$$

4.1 Stability and Hopf bifurcation of the delayed system

There are two cases to be investigated.

4.1.1 Case I: $\tau_1 = 0$ and $\tau_2 > 0$

For $\tau_1 = 0$ and $\tau_2 > 0$, the characteristic equation is

$$\psi(\xi, \tau_2) = \xi^5 + m_1\xi^4 + m_2\xi^3 + m_3\xi^2 + m_4\xi + m_5e^{-\xi\tau_2}(n_1\xi^4 + n_2\xi^3 + n_3\xi^2 + n_4\xi + n_5) = 0, \quad (17)$$

where

$$\begin{aligned}
m_1 &= L_1, \quad m_2 = L_2 + M_2, \quad m_3 = L_3 + M_3, \quad m_4 = L_4 + M_4, \quad m_5 = L_5 + M_5, \\
n_1 &= K_1, \quad n_2 = K_2 + Q_2, \quad n_3 = K_3 + Q_3, \quad n_4 = K_4 + Q_4, \quad n_5 = K_5 + Q_5.
\end{aligned}$$

For Hopf bifurcation to occur, we need to find a purely imaginary root of (17). Let us assume $\xi = i\omega$, $\omega > 0$, to be a purely imaginary root of (17). Putting $\xi = i\omega$ in (17), and separating real and imaginary parts, we get

$$\begin{aligned}
m_1\omega^4 - m_3\omega^2 + m_5 &= -(n_1\omega^4 - n_3\omega^2 + n_5) \cos \omega\tau_2 - (-n_2\omega^3 + n_4\omega) \sin \omega\tau_2, \\
\omega^5 - m_2\omega^3 + m_4\omega &= (n_1\omega^4 - n_3\omega^2 + n_5) \sin \omega\tau_2 - (-n_2\omega^3 + n_4\omega) \cos \omega\tau_2.
\end{aligned} \quad (18)$$

Squaring and adding the two equations of (18), we obtain that

$$\omega^{10} + p_1\omega^8 + p_2\omega^6 + p_3\omega^4 + p_4\omega^2 + p_5 = 0, \quad (19)$$

where

$$\begin{aligned} p_1 &= m_1^2 - 2m_2 - n_1^2, & p_2 &= m_2^2 + 2m_4 - 2m_1m_3 - n_2^2 + 2n_1n_3, \\ p_3 &= m_3^2 + 2m_1m_5 - 2m_4m_2 - 2n_1n_5 + 2n_4n_2 - n_3^2, \\ p_4 &= -2m_3m_5 + m_4^2 + 2n_3n_5 - n_4^2, & p_5 &= m_5^2 - n_5^2. \end{aligned}$$

Letting $\xi^2 = l$, the equation (19) becomes

$$H(l) = l^5 + p_1l^4 + p_2l^3 + p_3l^2 + p_4l + p_5 = 0. \quad (20)$$

Now, for later use, we define:

$$\begin{aligned} a_1 &= -\frac{6}{25}p_1^2 + \frac{3}{5}p_2, & b_1 &= -\frac{6}{25}p_1p_2 + \frac{2}{5}p_3 + \frac{8}{125}p_1^3, \\ c_1 &= -\frac{3}{625}p_1^4 + \frac{3}{125}p_1^2p_2 - \frac{2}{25}p_1p_3 + \frac{1}{5}p_4, & \Delta_0 &= a_1^2 - 4c_1, \\ a_2 &= -\frac{1}{3}a_1 - 4c_1, & b_2 &= -\frac{2}{27}a_1^3 + \frac{8}{3}a_1c_1 - b_1^2, \\ \Delta_1 &= a_1 - 4c_1, & d_0 &= \sqrt[3]{-\frac{b_2}{2} + \sqrt{\Delta_1}} + \sqrt[3]{-\frac{b_2}{2} - \sqrt{\Delta_1}} + \frac{a_1}{3}, \\ \Delta_2 &= -d_0 - a_1 + \frac{2b_1}{\sqrt{d_0 - a_1}}, & \Delta_3 &= -d_0 - a_1 - \frac{2b_1}{\sqrt{d_0 - a_1}}. \end{aligned} \quad (21)$$

Applying the results on the distribution of roots for an equation of degree five, as derived in [34], we get Lemma 5.

Lemma 5. *For the polynomial equation (20), the following results hold:*

- (a) *If $p_5 < 0$, then equation (20) will have at least one positive root.*
- (b) *Suppose $p_5 \geq 0$ and $b_1 = 0$.*
 - (i) *If $\Delta_0 < 0$, then equation (20) has no positive real root.*
 - (ii) *If $\Delta_0 \geq 0$ and $a_1 \geq 0$ and $c_1 > 0$, then (20) has no positive real root.*
 - (iii) *If (i) and (ii) are not satisfied, then (20) has a positive real root if and only if there exists at least one positive $l \in \{l_1, l_2, l_3, l_4\}$ such that $H(l) \leq 0$, where*

$$l_i = \delta_i - \frac{p_1}{5}, \quad i = 1, 2, 3, 4,$$

and

$$\begin{aligned} \delta_1 &= \sqrt{\frac{-a_1 + \sqrt{\Delta_0}}{2}}, & \delta_2 &= -\sqrt{\frac{-a_1 + \sqrt{\Delta_0}}{2}}, \\ \delta_3 &= \sqrt{\frac{-a_1 - \sqrt{\Delta_0}}{2}}, & \delta_4 &= -\sqrt{\frac{-a_1 - \sqrt{\Delta_0}}{2}}. \end{aligned}$$

- (c) *Suppose that $p_5 \geq 0$, $b_1 \neq 0$ and $d_0 > b_1$.*
 - (i) *If $\Delta_2 < 0$ and $\Delta_3 < 0$, then (20) has no positive real root.*
 - (ii) *If (i) is not satisfied, then (20) has a positive real root if and only if there exists at least one positive $l \in \{l_1, l_2, l_3, l_4\}$ such that $H(l) \leq 0$, where*

$$l_i = \delta_i - \frac{p_1}{5}, \quad i = 1, 2, 3, 4,$$

and

$$\begin{aligned}\delta_1 &= \frac{-\sqrt{d_0 - a_1} + \sqrt{\Delta_2}}{2}, & \delta_2 &= \frac{-\sqrt{d_0 - a_1} - \sqrt{\Delta_2}}{2}, \\ \delta_3 &= \frac{-\sqrt{d_0 - a_1} + \sqrt{\Delta_3}}{2}, & \delta_4 &= \frac{-\sqrt{d_0 - a_1} - \sqrt{\Delta_3}}{2}.\end{aligned}$$

(d) Assume that $\Delta_0 \geq 0$ and $b_1 \neq 0$. Then, (20) has a positive real root if and only if

$$\frac{b_1}{4(a_1 - d_0)} + \frac{1}{2}d_0 = 0, \quad \bar{l} > 0, \quad H(\bar{l}) \leq 0,$$

where $\bar{l} = b_1/2(a_1 - d_0) - \frac{1}{5}p_1$.

Without loss of generality, we have assumed that equation (20) has r positive roots with $r \in \{1, 2, 3, 4, 5\}$, denoted by $l_k, k = 1, 2, \dots, r$. Then, equation (19) has r positive roots, say $\omega_k = \sqrt{l_k}, k = 1, 2, \dots, r$. Therefore, $i \pm \omega_k$ is a pair of purely imaginary roots of (17). Now, using equation (18), we derive

$$\begin{aligned}\sin(\tau_2 \eta) &= \frac{(\omega^5 - m_2 \omega^3 + m_4 \omega)(n_1 \omega^4 - n_3 \omega^2 + n_5)}{(n_1 \omega^4 - n_3 \omega^2 + n_5)^2 + (n_2 \omega^3 - n_4 \omega)^2} - \frac{(m_1 \omega^4 - m_3 \omega^2 + m_5)(-n_2 \omega^3 + n_4 \omega)}{(n_1 \omega^4 - n_3 \omega^2 + n_5)^2 + (n_2 \omega^3 - n_4 \omega)^2} \\ &= \gamma(\eta).\end{aligned}\tag{22}$$

If equation (19) has at least one positive root, say ω_0 , then (17) will have a pair of purely imaginary roots $\pm i \omega_0$ corresponding to the delay τ_2^* . Without loss of generality, we assume that (19) has ten positive real roots, which are denoted as $\eta_1, \eta_2, \dots, \eta_{10}$, respectively. For every fixed $\omega_k, k = 1, 2, \dots, 10$, the corresponding critical values of time delay τ_2 are

$$\tau_{2,n}^{(j)} = \frac{1}{\omega_k} \arcsin \gamma(\eta) + \frac{2\pi j}{\omega_k}, \quad j = 0, 1, 2, \dots$$

Let

$$\tau_2^* = \min \left\{ \tau_{2,k}^{(j)} \right\}, \quad \omega_0 = \omega_k |_{\tau_2 = \tau_2^*}, \quad k = 1, 2, \dots, r, \quad j = 0, 1, 2, \dots\tag{23}$$

Taking the derivative of (17) with respect to τ_2 , it is easy to obtain that

$$\left(\frac{d\xi}{d\tau_2} \right)^{-1} = -\frac{5\xi^4 + 4m_1\xi^3 + 3m_2\xi^2 + 2m_3\xi + m_4}{\xi(\xi^5 + m_1\xi^4 + m_2\xi^3 + m_3\xi^2 + m_4\xi + m_5)} + \frac{4n_1\xi^3 + 3n_2\xi^2 + 2n_3\xi + n_4}{\xi(n_1\xi^4 + n_2\xi^3 + n_3\xi^2 + n_4\xi + n_5)} - \frac{\tau_2}{\xi}.\tag{24}$$

Thus, we have

$$\text{sign} \left[\frac{d \operatorname{Re}\{\xi(\tau_2)\}}{d\tau_2} \right]_{\tau_2 = \tau_{2,k}^{(j)}} = \text{sign} \left[\operatorname{Re} \left(\frac{d\xi}{d\tau_2} \right) \right]_{\xi = i\omega_0}.\tag{25}$$

Using (19), and after simple calculations, it can be shown that for $\xi = i\omega_0$ one has

$$\text{sign} \left[\frac{d \operatorname{Re}\{\xi(\tau_2)\}}{d\tau_2} \right]_{\tau_2 = \tau_{2,k}^{(j)}} = \text{sign} \left[\frac{H'(l_k)}{\omega_0^2(n_2\omega_0^2 - n_4)^2 + (n_1\omega_0^4 - n_3\omega_0^2 + n_5)^2} \right].\tag{26}$$

We conclude that $\frac{d \operatorname{Re}\{\xi(\tau_2)\}}{d\tau_2} |_{\tau_2 = \tau_{2,k}^{(j)}}$ and $H'(l_k)$ have the same sign.

We summarize the above discussion in the following theorem.

Theorem 6. Let ω_0 and τ_2^* be defined by (23). Consider the conditions

(i) $p_5 < 0$;

(ii) $p_5 \geq 0, b_1^* = 0, \Delta_0 \geq 0$ and $a_1^* < 0$ or $c_1^* \leq 0$ and there exists $l^* \in \{l_1, l_2, l_3, l_4\}$ such that $l^* > 0$ and $H(l^*) \leq 0$;

(iii) $p_5 \geq 0$, $b_1^* \neq 0$, $d_0^* > b_1^*$ and $\Delta_2 \geq 0$ or $\Delta_3 \geq 0$ and there exist $l^* \in \{l_1, l_2, l_3, l_4\}$ such that $l^* > 0$ and $H(l^*) \leq 0$;

(iv) if $\Delta_0 \geq 0$ and $b_1^* \neq 0$, then (20) has a positive real root if and only if $b_1^*/4(a_1^* - d_0^*) + \frac{1}{2}d_0^* = 0$ and $\bar{l} > 0$ and $H(\bar{l}) \leq 0$, where $\bar{l} = b_1^*/2(a_1^* - d_0^*) - \frac{1}{5}p_1$.

The following holds:

1. If none of conditions (i), (ii), (iii) and (iv) are satisfied, then the equilibrium E^* is locally asymptotically stable for any $\tau_2 \geq 0$.
2. If any of the conditions (i), (ii), (iii) or (iv) is satisfied, then the equilibrium E^* is locally asymptotically stable for $\tau_2 \in [0, \tau_2^*)$.
3. If one of the conditions (i), (ii), (iii) or (iv) holds and $H(\bar{l}_0) \neq 0$, then E^* undergoes Hopf bifurcation as τ_2 passes through the critical value τ_2^* .

4.1.2 Case II: $\tau_1 > 0$ and $\tau_2 = 0$

At the endemic equilibrium E^* , the characteristic equation has delay-dependent coefficients (i.e., for $\tau_1 > 0$) and it is quite involved. Therefore, it is difficult to obtain analytically information on the nature of the eigenvalues and on the conditions for occurrence of stability switches. However, the nature of the eigenvalues can be investigated at the endemic state through numerical simulations, which we do in Section 5.

5 Numerical Simulations

In this section, we provide some numerical simulations for illustrating the dynamics of the system. The numerical simulation of model (2) is plotted with the basic model parameters as in Table 1. In Figure 2, we plot the solutions of the model variables corresponding to uninfected epithelial cells (T), infected epithelial cells (I), SARS-CoV-2 virus (V), ACE2 receptor of epithelial cells (E), and CTL responses (C) for the non-delayed and delayed system. The blue line indicates the non-delayed system whereas the red line represents the delayed system with $\tau_1 = 5$, keeping $\tau_2 = 0$. The initial point is obtained by perturbing T from the non-trivial equilibrium values E_1 given by $(\tilde{T}, \tilde{I}, \tilde{V}, \tilde{E}, \tilde{C}) = (46.78, 2.91, 14.47, 9.8, 1.05)$, using the set of parameters from Table 1. In Figure 2, we choose the initial conditions as $T(\theta) = 45$, $I(\theta) = 4$, $V(\theta) = 20$, $E(\theta) = 9.5$, $C(\theta) = 2$ for $\theta \in (-\tau, 0]$. When $\tau_1 = \tau_2 = 0$ days, the non-trivial equilibrium E is locally asymptotically stable. But in presence of a delay, the system attains its lower concentration with respect to p . The system shows similar behaviors with respect to the parameter q (see Figure 3). Thus, the lytic and nonlytic effect on the model in presence of delay shows almost similar behaviors.

Figures 4 and 6 show that increasing the value of the delay makes the oscillation in the system solution and it persists for a longer period of time. The parameter values used in $H(l)$ have one positive simple real root and the corresponding value of τ_2 is days. Our simulations are consistent with the theoretical findings. When $\tau_1 = \tau_2 = 0$, the endemic equilibrium E^* is locally asymptotically stable. The initial oscillation persist for a longer period for an increasing value of the delay τ_2 and the value of the delay passes through its critical value (see Figures 5 and 7), then the system attains Hopf bifurcation.

6 Discussion

We have studied the CTL responses on SARS-CoV-2 infected epithelial cells through mathematical modeling. In our proposed model, we have considered a delay in the disease transmission term and a CTL proliferation term. We have studied the delay-induced system both analytically and numerically.

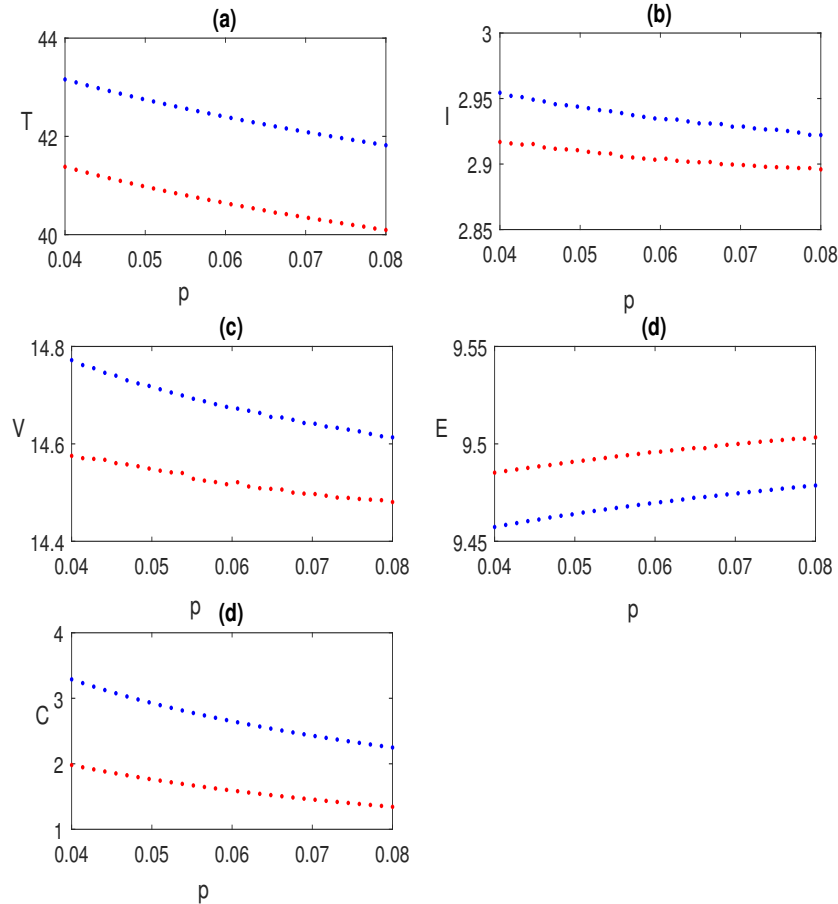


Figure 2: Effect of parameter p (the efficacy of the lytic effect) on the system when $\tau_1 = 0 = \tau_2$. The other parameter values are given in Table 1.

Our analytical findings reveal that the non-delayed system attains its infection-free state when the basic reproduction number R_0 given by (4) is less than 1 and that the system moves to the infected state when $R_0 > 1$. We have also witnessed that the infected equilibrium E^* becomes unstable as the time delay increases. Also, it is observed that as the time delay increases the system remains unstable or it may cycle through an infinite sequence of regions, alternately locally asymptotically stable and unstable. Again, we found the threshold value of the delays for which the system undergoes Hopf bifurcation.

Numerical findings of the model confirm our analytical results. We found for the estimated parameter values, as mentioned in Table 1, that the infected state becomes unstable as the time delay increases but did not stabilize again at its higher values. In the unstable region, the system shows an oscillatory behavior at the critical time delay. Our analysis also demonstrates that the time delay, as well as the parameters p and q , play a crucial role in the stability of the system. The competition between the parameters p , q , and the delays to control the system depends on their respective numerical values.

Summarizing, our analytical, as well as numerical findings, tell us that increasing the immune time delay τ_2 in the system causes always an increasing of oscillations and instability while, in contrast, the incubation delay τ_1 has a stabilizing role.

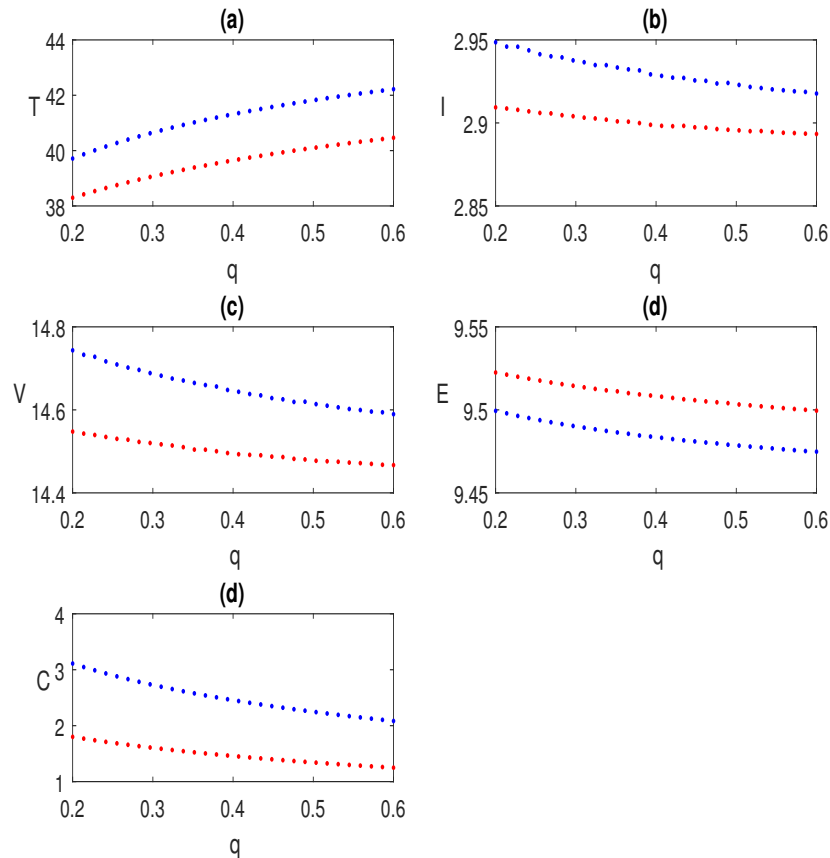


Figure 3: Effect of parameter q (the efficacy of the nonlytic effect) on the system when $\tau_1 = 0 = \tau_2$. The other parameter values are given in Table 1.

7 Conclusion

Time delay models are important tools in the modeling of infectious diseases because they allow for more realistic representations of the spread and course of infection. In this study, a time delay model of COVID-19 has been proposed and analyzed. 'Latent period' and the 'time for immune response' have been considered as the time delay parameters for this study. We demonstrated that the delay in immune response has a destabilizing effect, whereas latent delay contributes to stabilization. The proposed time delay model is more realistic. The outcomes of this study may be beneficial for appropriate treatment of COVID-19.

Data availability

The data supporting the findings of this study are available within the article.

Acknowledgements

Torres was supported by FCT through project UIDB/04106/2020 (CIDMA). The authors are thankful to a reviewer for useful comments.

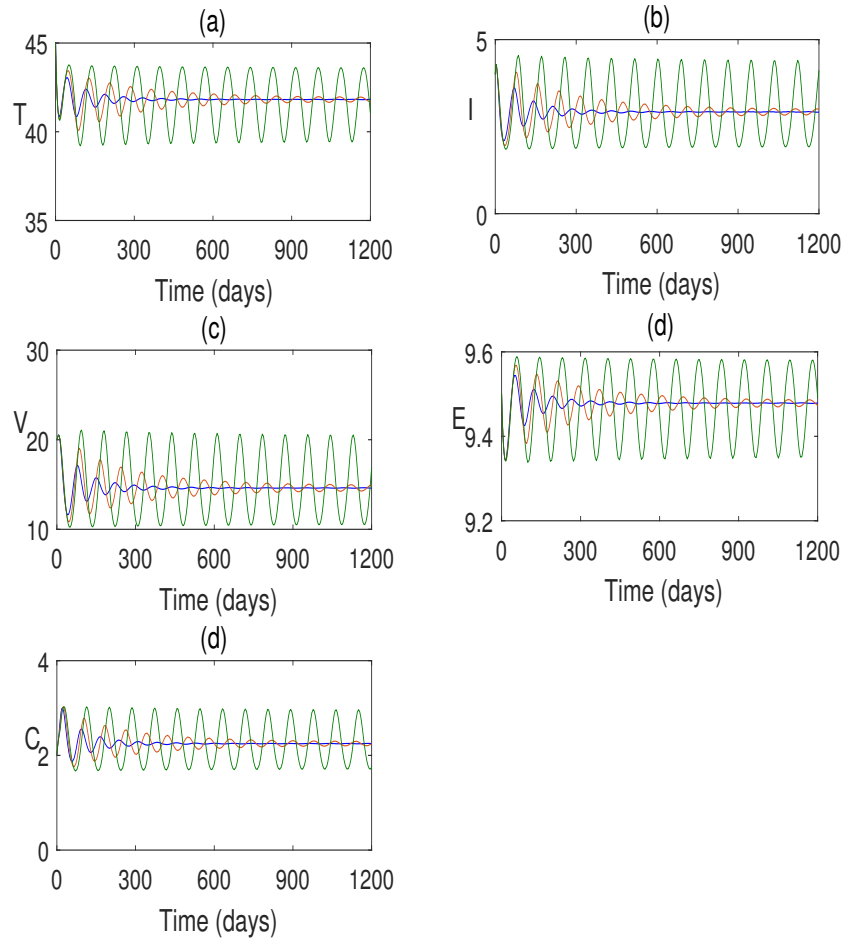


Figure 4: Numerical solution of the system with $\tau_1 = 0$ and for different values of τ_2 . The other parameter values are given in Table 1.

References

- [1] 2-DG, Dr. Reddy's Laboratories, Antiviral and anti-inflammatory drug, Accessed February 19, 2022. <https://www.drreddys.com/2dg>
- [2] CDC, Centers for Disease Control and Prevention, Different COVID-19 Vaccines, Accessed January 21, 2022. <https://www.cdc.gov/coronavirus/2019-ncov/vaccines/different-vaccines.html>
- [3] P. Agarwal, J. J. Nieto, M. Ruzhansky and D. F. M. Torres, Analysis of Infectious Disease Problems (Covid-19) and Their Global Impact, Springer Nature, Singapore, 2021.
- [4] R. K. Rai, S. Khajanchi, P. K. Tiwari, E. Venturino and A. K. Misra, Impact of social media advertisements on the transmission dynamics of COVID-19 pandemic in India, *J. Appl. Math. Comput.* **68** (2022), 19–44.
- [5] P. K. Tiwari, R. K. Rai, S. Khajanchi, R. K. Gupta and A. K. Misra, Dynamics of coronavirus pandemic: effects of community awareness and global information campaigns, *Eur. Phys. J. Plus* **136** (2021), Art. 994.
- [6] P. Samui, J. Mondal and S. Khajanchi, A mathematical model for COVID-19 transmission dynamics with a case study of India, *Chaos Solitons Fractals* **140** (2020), 110173, 11 pp.

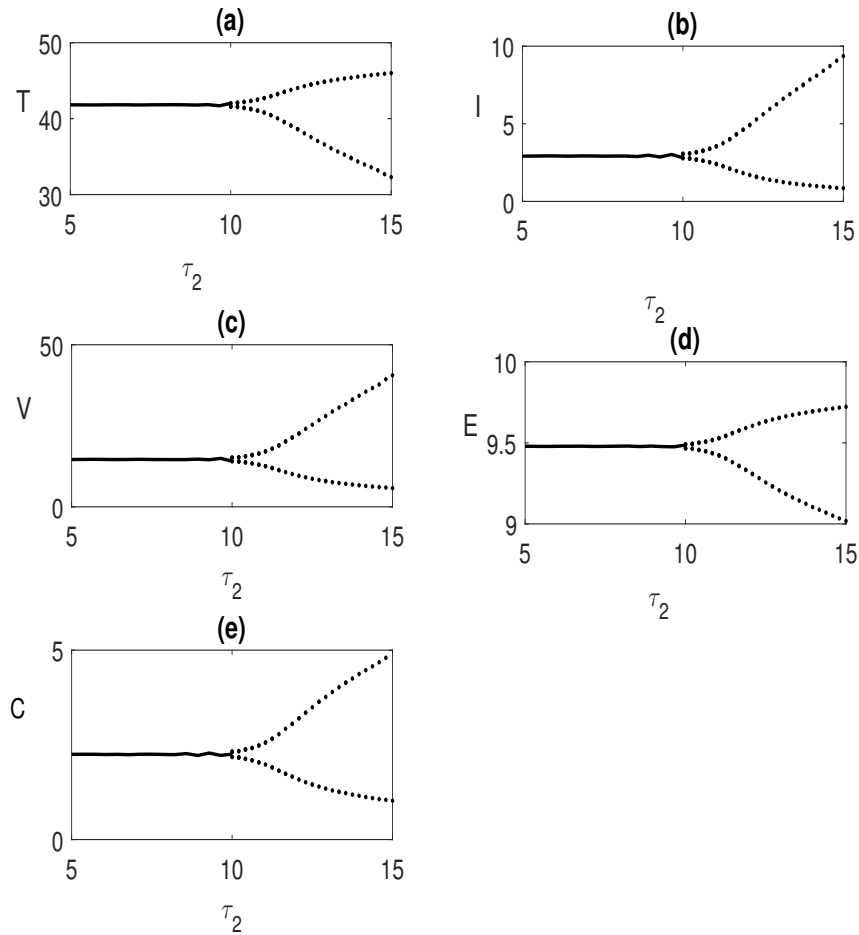


Figure 5: Bifurcation diagram of the system taking τ_2 as the bifurcation parameter and $\tau_1 = 0$. Other parameters are the same as for Figure 4. The solid line indicates the stable endemic equilibrium.

- [7] J. Mondal, P. Samui and A. N. Chatterjee, Optimal control strategies of non-pharmaceutical and pharmaceutical interventions for COVID-19 control, *J. Interdiscip. Math.* **24** (2021), no 1, 125–153.
- [8] B. Rahman, S. H. A. Khoshnaw, G. O. Agaba and F. Al Basir, How containment can effectively suppress the outbreak of COVID-19: A mathematical modeling, *Axioms* **10** (2021), no. 3, Art. 204, 13 pp.
- [9] S. Tang, W. Ma and P. Bai, A novel dynamic model describing the spread of the MERS-CoV and the expression of dipeptidyl peptidase 4, *Comput. Math. Methods Med.* **2017** (2017), Art. ID 5285810, 6 pp.
- [10] A. K. Srivastav, P. K. Tiwari, P. K. Srivastava, M. Ghosh and Y. Kang, A mathematical model for the impacts of face mask, hospitalization and quarantine on the dynamics of COVID-19 in India: deterministic vs. stochastic, *Math. Biosci. Eng.* **18** (2021), no. 1, 182–213.
- [11] M. Majumder, P. K. Tiwari and S. Pal, Impact of saturated treatments on HIV-TB dual epidemic as a consequence of COVID-19: optimal control with awareness and treatment, *Nonlinear Dyn.* **109** (2022), 143–176.

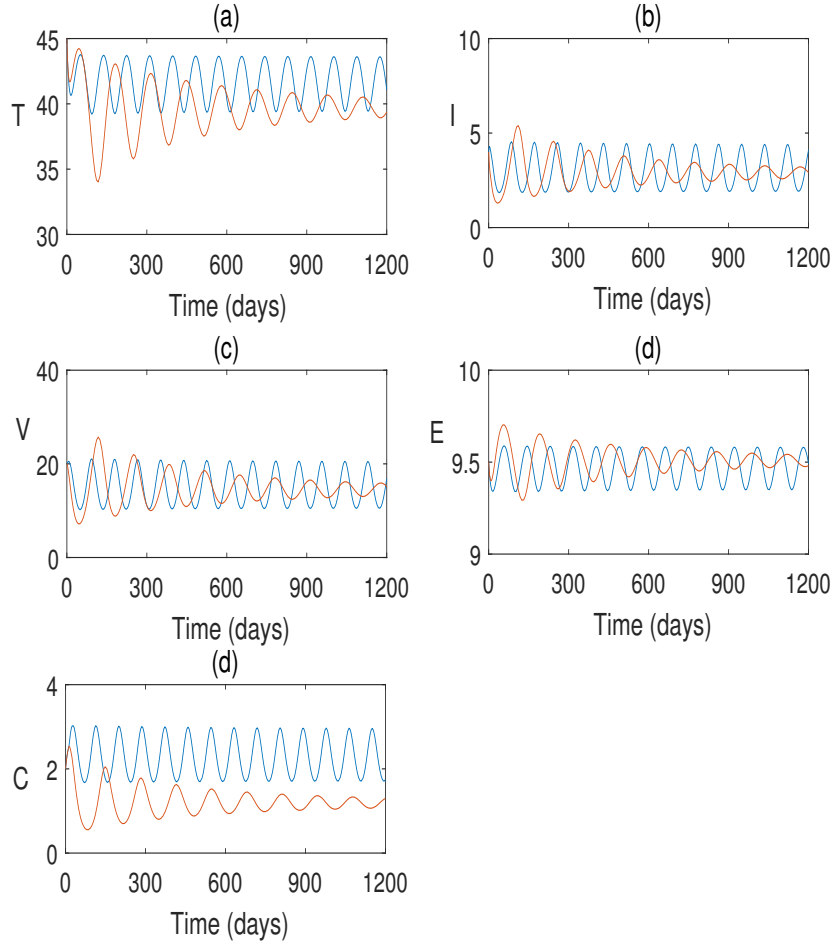


Figure 6: Numerical solution of the system with $\tau_2 = 12$ and for different values of τ_1 . The blue line is for $\tau_1 = 6$ and the red line is for $\tau_1 = 1$.

- [12] H. Zine, A. Boukhouima, E. M. Lotfi, M. Mahrouf, D. F. M. Torres and N. Yousfi, A stochastic time-delayed model for the effectiveness of Moroccan COVID-19 deconfinement strategy, *Math. Model. Nat. Phenom.* **15** (2020), Paper No. 50, 14 pp.
- [13] M. Mahrouf, A. Boukhouima, H. Zine, E. M. Lotfi, D. F. M. Torres and N. Yousfi, Modeling and forecasting of COVID-19 spreading by delayed stochastic differential equations, *Axioms* **10** (2021), no. 1, Art. 18, 16 pp.
- [14] F. Ndaïrou, I. Area, J. J. Nieto, C. J. Silva and D. F. M. Torres, Fractional model of COVID-19 applied to Galicia, Spain and Portugal, *Chaos Solitons Fractals* **144** (2021), Paper No. 110652, 7 pp.
- [15] C.J. Silva, C. Cruz, D.F.M. Torres, A.P. Munuzuri, A. Carballosa, I. Area, J.J. Nieto, R. Fonseca-Pinto, R. Passadouro da Fonseca, E. Soares dos Santos, W. Abreu and J. Mira, Optimal control of the COVID-19 pandemic: controlled sanitary deconfinement in Portugal, *Scientific Reports* **11** (2021), Art. 3451, 15 pp.
- [16] J. Mondal, P. Samui and A. N. Chatterjee, Dynamical demeanour of SARS-CoV-2 virus undergoing immune response mechanism in COVID-19 pandemic, *Eur. Phys. J. Spec. Top.* **231** (2022), 3357–3370.

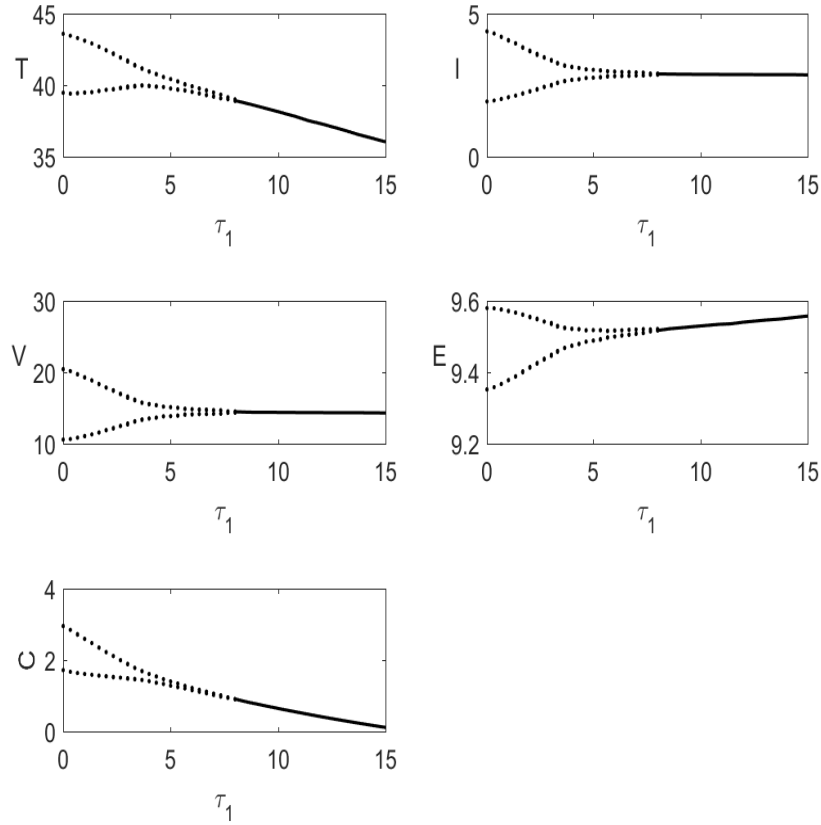


Figure 7: Bifurcation diagram of the system taking τ_1 as the bifurcation parameter ($\tau_2 = 12$). The solid line indicates the stable endemic equilibrium.

- [17] C. J. Silva, G. Cantin, C. Cruz, R. Fonseca-Pinto, R. Passadouro da Fonseca, E. Soares dos Santos and D. F. M. Torres, Complex network model for COVID-19: human behavior, pseudo-periodic solutions and multiple epidemic waves, *J. Math. Anal. Appl.* **514** (2022), no. 2, Art. 125171, 25 pp.
- [18] R. K. Rai, P. K. Tiwari and S. Khajanchi, Modeling the influence of vaccination coverage on the dynamics of COVID-19 pandemic with the effect of environmental contamination, *Math. Methods Appl. Sci.* **46** (2023), no. 12, 12425–12453.
- [19] S. Qureshi and A. Yusuf, Fractional derivatives applied to MSEIR problems: Comparative study with real world data, *Eur. Phys. J. Plus* **134** (2019), Art. 171, 13 pp.
- [20] S. Qureshi, A. Yusuf, A. A. Shaikh and M. Inc, Transmission dynamics of varicella zoster virus modeled by classical and novel fractional operators using real statistical data, *Phys. A* **534** (2019), 122149, 22 pp.
- [21] P. K. Roy, A. N. Chatterjee and X.-Z. Li, The effect of vaccination to dendritic cell and immune cell interaction in HIV disease progression, *Int. J. Biomath.* **9** (2016), no. 1, 1650005, 20 pp.

- [22] A. N. Chatterjee and P. K. Roy, Anti-viral drug treatment along with immune activator IL-2: a control-based mathematical approach for HIV infection, *Internat. J. Control* **85** (2012), no. 2, 220–237.
- [23] P. K. Roy, A. N. Chatterjee, D. Greenhalgh and Q. J. A. Khan, Long term dynamics in a mathematical model of HIV-1 infection with delay in different variants of the basic drug therapy model, *Nonlinear Anal. Real World Appl.* **14** (2013), no. 3, 1621–1633.
- [24] S. Ghosh, A. N. Chatterjee, P. K. Roy, N. Grigorenko, E. Khailov and E. Grigorieva, Mathematical modeling and control of the cell dynamics in leprosy, *Comput. Math. Model.* **32** (2021), no. 1, 52–74.
- [25] K. Allali, S. Harroudi and D. F. M. Torres, Optimal control of an HIV model with a trilinear antibody growth function, *Discrete Contin. Dyn. Syst. Ser. S* **15** (2022), no. 3, 501–518.
- [26] B. Wanga, J. Mondal, P. Samui, A. N. Chatterjee and A. Yusuf, Effect of an antiviral drug control and its variable order fractional network in host COVID-19 kinetics, *Eur. Phys. J. Spec. Top.* **231** (2022), 1915–1929.
- [27] A. N. Chatterjee and F. Al Basir, A model for SARS-CoV-2 infection with treatment, *Comput. Math. Method Med.* **2020** (2020), Art. ID 1352982, 11 pp.
- [28] E. A. Hernandez-Vargas and J. X. Velasco-Hernandez, In-host mathematical modelling of COVID-19 in humans, *Annu. Rev. Control* **50** (2020), 448–456.
- [29] S. Wang, Y. Pan, Q. Wang, H. Miao, A. N. Brown and L. Rong, Modeling the viral dynamics of SARS-CoV-2 infection, *Math. Biosci.* **328** (2020), 108438, 12 pp.
- [30] A. N. Chatterjee and B. Ahmad, A fractional-order differential equation model of COVID-19 infection of epithelial cells, *Chaos Solitons Fractals* **147** (2021), Paper No. 110952, 6 pp.
- [31] A. N. Chatterjee, F. Al Basir, M. A. Almuqrin, J. Mondal and I. Khan, SARS-CoV-2 infection with lytic and non-lytic immune responses: A fractional order optimal control theoretical study, *Results Phys.* **26** (2021), Art. 104260, 9 pp.
- [32] T. Abraha, F. Al Basir, L. L. Obsu and D. F. M. Torres, Controlling crop pest with a farming awareness based integrated approach and optimal control, *Comput. Math. Methods* **3** (2021), no. 6, Paper No. e1194, 24 pp.
- [33] T. Abraha, F. Al Basir, L. L. Obsu and D. F. M. Torres, Pest control using farming awareness: impact of time delays and optimal use of biopesticides, *Chaos Solitons Fractals* **146** (2021), Paper No. 110869, 11 pp.
- [34] T. Zhang, H. Jiang and Z. Teng, On the distribution of the roots of a fifth degree exponential polynomial with application to a delayed neural network model, *Neurocomputing* **72** (2009), no. 4-6, 1098–1104.